

# Average-Intensity Reconstruction and Wiener Reconstruction of Bioelectric Current Distribution Based on Its Estimated Covariance Matrix

Kensuke Sekihara, *Member, IEEE*, and Bernhard Scholz

**Abstract**—This paper proposes two methods for reconstructing current distributions from biomagnetic measurements. Both of these methods are based on estimating the source-current covariance matrix from the measured-data covariance matrix. One method is the reconstruction of average current intensity distributions. This method first estimates the source-current covariance matrix and, using its diagonal terms, it reconstructs current intensity distributions averaged over a certain time. Although the method does not reconstruct the orientation of each current element at each time instant, it can retrieve information regarding the current time-averaged intensity at each voxel location using extremely low SNR data. The second method is Wiener reconstruction using the estimated source-current covariance matrix. Unlike the first method, this Wiener reconstruction can provide a current distribution with its orientation at each time instant. Computer simulation shows that the Wiener method is less affected by the choice of the regularization parameter, resulting in a method that is more effective than the conventional minimum-norm method when the SNR of the measurement is low.

## I. INTRODUCTION

**R**ECONSTRUCTING bioelectric current distributions in a human brain from the biomagnetic field measured on the brain surface is expected to provide functional brain images and thus has attracted a great deal of interest. A well-known algorithm to reconstruct current distributions [1], [2], [3] is based on the pseudoinversion of the lead field matrix, which represents each detector's sensitivity pattern over the reconstruction region. In this reconstruction, one should first calculate the lead field matrix. Then, the Moore-Penrose pseudoinversion of the lead field matrix should be calculated and multiplied with the measured magnetic field data to obtain the minimum norm estimates of the primary current distributions. Thus, this reconstruction method is often called the minimum-norm reconstruction. In this reconstruction, to calculate the Moore-Penrose pseudoinverse, the matrix regularization is usually used and the values of the regularization parameter must be empirically determined.

One serious drawback of the minimum-norm reconstruction is that the results are significantly affected by the values of the regularization parameter. This is especially true when the signal-to-noise ratio (SNR) of the measurements is low. Unfortunately, the biomagnetic field from a human brain is

so weak that such low SNR situations are very common. For measurements of evoked neuromagnetic fields, the SNR can be improved to some extent by averaging signals that are measured synchronized with the stimulus. This, however, inevitably causes prolonged measurement time. Therefore, the amount of averaging is limited to 100–200 times. For the measurements of spontaneous brain signals, it is generally difficult to achieve SNR improvements by signal averaging. Such spontaneous signals are believed to have a strong relationship with many functions in the human brain [4], as well as brain malfunctions such as epilepsy [5]. Accordingly, a reconstruction method that is not very sensitive to the SNR is highly desirable for developing brain functional imaging.

This paper proposes two methods for reconstructing current distributions that are more effective than the conventional minimum-norm reconstruction method in low SNR situations. Both methods utilize time information by calculating the measured-data covariance matrix. One method is reconstruction of average-current-intensity distributions. This method can reconstruct current intensity distributions averaged over a certain time period. Although this method does not reconstruct the orientation of each current element at each time instant, the method can retrieve the information regarding the average intensity of the primary current at each voxel location using extremely low SNR data.

The second method is the Wiener reconstruction based on the estimated signal-source covariance matrix. Unlike the first method, the Wiener reconstruction method can provide the current distribution with its orientation at each time instant. Our computer simulation shows that the Wiener method is less affected by the choice of the regularization parameter, and more effective than the conventional minimum-norm method when the SNR of the measurement is low.

## II. METHOD

### A. General Description

Let us define the component of the magnetic field measured by the  $m$ th detector coil as  $B_m$ , and a vector  $\mathbf{B} = (B_1, B_2, \dots, B_M)^T$  is defined as a set of measured data. Here,  $M$  is the total number of detector coils and the superscript  $T$  indicates the matrix transpose. Let us also define the primary current distribution, which is the source of the magnetic field, as a vector  $\mathbf{f} = (f_1, f_2, \dots, f_{3N})^T$ . Here,  $N$  is the total number of voxels and the  $x$ ,  $y$ , and  $z$  components of

Manuscript received July 31, 1992; revised August 26, 1994.

K. Sekihara is with Central Research Laboratory, Hitachi, Limited, Kokubunji, Tokyo 185, Japan.

B. Scholz is with Siemens AG, Medical Engineering Group, D91 052 Erlangen, Germany.

IEEE Log Number 9407582.

the primary current located at the  $k$ th voxel are assigned to  $f_{3(k-1)+1}$ ,  $f_{3(k-1)+2}$ , and  $f_{3(k-1)+3}$ , respectively. Representing the additive noise contained in the measured data as a vector  $\mathbf{n}$ , the relationship between  $\mathbf{B}$  and  $\mathbf{f}$  can be expressed as

$$\mathbf{B} = \mathbf{L}\mathbf{f} + \mathbf{n}. \quad (1)$$

Here,  $\mathbf{L}$  is an  $M \times (3N)$  matrix and its elements,  $L_{m, 3(k-1)+1}$ ,  $L_{m, 3(k-1)+2}$ , and  $L_{m, 3(k-1)+3}$ , represent the sensitivity of the  $m$ th detector to the  $x$ ,  $y$ , and  $z$  components of the primary current at the  $k$ th voxel. This matrix  $\mathbf{L}$  is called the lead field matrix.

### B. Conventional Minimum-Norm Reconstruction

In conventional reconstruction, current estimates  $\hat{\mathbf{f}}$  are obtained by minimizing the cost function  $E = \|\mathbf{B} - \hat{\mathbf{B}}\|^2$ , where  $\hat{\mathbf{B}} = \mathbf{L}\hat{\mathbf{f}}$ . This minimization has a well-known solution using the Moore-Penrose generalized inverse [6]  $L^-$ . Namely,

$$\hat{\mathbf{f}} = L^- \mathbf{B}. \quad (2)$$

Here, for the underdetermined cases,  $M < 3N$ ,  $L^-$  is given by  $L^- = L^T(LL^T)^{-1}$ . This conventional method using (2) is sometimes called the least-squares minimum-norm estimation method.

In practice, to avoid the numerical instability associated with the matrix inversion, matrix regularization is often used, and the generalized inverse  $L^-$  is calculated from [7]

$$L^- = L^T(LL^T + \gamma I)^{-1}, \quad (3)$$

where  $I$  is the unit matrix and  $\gamma$  is the predetermined regularization parameter. It should be noted that the estimates obtained using (2) and (3) minimize the cost function expressed as [8]

$$E = \|\mathbf{B} - \hat{\mathbf{B}}\|^2 + \gamma \|\hat{\mathbf{f}}\|^2, \quad (4)$$

instead of  $E = \|\mathbf{B} - \hat{\mathbf{B}}\|^2$ . Consequently, these estimates provide a trade-off between the minimization of the current norm  $\|\hat{\mathbf{f}}\|^2$  and the norm of the squared error term  $\|\mathbf{B} - \hat{\mathbf{B}}\|^2$ . Here, the parameter  $\gamma$  controls the degree of this trade-off.

The problem with the conventional minimum-norm method is that, when the SNR of the measured data is low, the reconstruction results are affected by the choice of this regularization parameter, as will be demonstrated in the next section. That is, a small value of  $\gamma$  tends to give severely distorted and almost meaningless results because the small eigenvalues of  $LL^T$  amplify the inaccuracy due to the noise in measured data. Conversely, a large  $\gamma$  tends to introduce spatial blur in reconstructed results. Thus, it is necessary to choose an appropriate value of  $\gamma$  that does not cause distortion with a minimum spatial blur.

Several methods have been investigated to determine the optimum value of  $\gamma$  on a certain mathematical basis. Such methods include those based on the Bayesian estimation theory [9], [10], and that using the criterion from  $\chi^2$  statistics [11], [12]. The  $\chi^2$  based method generally chooses  $\gamma$  larger than its optimum value, resulting in blurred reconstructions. The Bayesian methods tend to choose a value of  $\gamma$  smaller than that

chosen by the  $\chi^2$ -based method. The success of these Bayesian methods, however, depends on the measured data, and they are not very reliable in many cases. Thus, we often need to rely on a subjective criterion and determine the optimum  $\gamma$  in an empirical manner [12]. Since no method for determining the optimum  $\gamma$  value has been established and the allowance of this  $\gamma$  is not large when the SNR of the measured data is low, the conventional minimum-norm reconstruction is not very effective in such cases. The following subsections propose two methods that are more effective than the minimum-norm method in low SNR cases.

### C. Estimation of Source Current Covariance Matrix and Average-Intensity Reconstruction

The covariance matrix of the measured data denoted by  $\mathbf{D}$  is

$$\mathbf{D} = \langle \mathbf{B}\mathbf{B}^T \rangle = \begin{pmatrix} \langle B_1^2 \rangle & \langle B_1 B_2 \rangle & \cdots & \langle B_1 B_M \rangle \\ \langle B_2 B_1 \rangle & \langle B_2^2 \rangle & \cdots & \vdots \\ \vdots & \vdots & \ddots & \vdots \\ \langle B_M B_1 \rangle & \cdots & \cdots & \langle B_M^2 \rangle \end{pmatrix}. \quad (5)$$

Here,  $\langle \rangle$  indicates the time average. Let us assume that the source current distribution  $\mathbf{f}$  and the noise  $\mathbf{n}$  are not correlated. Thus, substituting (1) into (5), we can obtain

$$\mathbf{D} = \langle (\mathbf{L}\mathbf{f})(\mathbf{L}\mathbf{f})^T \rangle + \langle \mathbf{n}\mathbf{n}^T \rangle = \mathbf{L}\langle \mathbf{f}\mathbf{f}^T \rangle \mathbf{L}^T + \langle \mathbf{n}\mathbf{n}^T \rangle, \quad (6)$$

where  $\langle \mathbf{f}\mathbf{f}^T \rangle$  is the covariance matrix of a source-current distribution. Let us denote this covariance matrix as  $\mathbf{S}$ . Then,

$$\mathbf{S} = \langle \mathbf{f}\mathbf{f}^T \rangle = \begin{pmatrix} \langle f_1^2 \rangle & \langle f_1 f_2 \rangle & \cdots & \langle f_1 f_{3N} \rangle \\ \langle f_2 f_1 \rangle & \langle f_2^2 \rangle & \cdots & \vdots \\ \vdots & \vdots & \ddots & \vdots \\ \langle f_{3N} f_1 \rangle & \cdots & \cdots & \langle f_{3N}^2 \rangle \end{pmatrix}. \quad (7)$$

Denoting the noise covariance matrix as  $\mathbf{C} (= \langle \mathbf{n}\mathbf{n}^T \rangle)$ , we can get the relationship between  $\mathbf{S}$  and  $\mathbf{D}$ ,

$$\mathbf{D} = \mathbf{L}\mathbf{S}\mathbf{L}^T + \mathbf{C}. \quad (8)$$

Thus, the estimates of the covariance matrix of a source distribution,  $\hat{\mathbf{S}}$ , can be obtained from the noise and measured-data covariance matrices, i.e.,

$$\hat{\mathbf{S}} = L^- (\mathbf{D} - \mathbf{C}) (L^-)^T, \quad (9)$$

where  $L^-$  is the Moore-Penrose generalized inverse of  $\mathbf{L}$ , which is defined in (3). Here, the noise covariance  $\mathbf{C}$  should be estimated before the reconstruction.

The average squared intensity of the source current distribution,  $\langle f_i^2 \rangle$  where  $i = 1, 2, \dots, 3N$ , can be derived from the diagonal terms of its covariance matrix  $\mathbf{S}$ , as shown in (7). This reconstruction can be especially effective when applied to the source current estimation of spontaneous brain activities. Such activities, for example, human  $\alpha$  rhythms, often generate quasi-periodic magnetic signals, suggesting that the current sources fluctuate between positive and negative directions. Thus, simple summation of the measured field maps causes a cancellation of positive and negative signals and never achieves SNR improvement. On the other hand, our average-intensity reconstruction can achieve SNR improvement even

when the current sources fluctuate between positive and negative directions, because this method reconstructs the squared intensity of magnetic sources averaged over a certain time period. However, it loses the information about the current source moment at each time instant. Therefore, when this information is needed, Wiener reconstruction should be used as proposed in the next subsection.

#### D. Wiener Reconstruction Based on Estimated Source Covariance Matrix

The Wiener reconstruction is known to obtain the estimates that minimize the cost function [13],

$$E = \langle \|f - \hat{f}\|^2 \rangle. \quad (10)$$

The optimum estimates are known to be [13],

$$\hat{f} = \langle f B^T \rangle (B B^T)^{-1} B. \quad (11)$$

From (1), (8), and (9), we have  $\langle f B^T \rangle = S L^T = L^-(D - C)$ , assuming that  $\langle f n^T \rangle = 0$ . Thus, recalling  $\langle B B^T \rangle = D$ , (11) can be changed to

$$\hat{f} = L^-(D - C) D^{-1} B. \quad (12)$$

The above equation is used in our computer simulation in the next section. It is clear in this equation that, when the SNR is so high that the noise covariance  $C$  is negligible compared with  $D$ , the Wiener reconstruction becomes equal to the conventional minimum-norm reconstruction,  $\hat{f} = L^- B$ .

This Wiener reconstruction incorporates the information on the noise and the signal-source covariance matrices. It is known, in the field of image restoration [8], [13], that the Wiener method gives better results than the conventional minimum-norm method when the SNR of the measured data is low. The computer simulations described in the next section show that this Wiener reconstruction is also more effective than the conventional minimum-norm method in the biomagnetic inverse problem.

### III. COMPUTER SIMULATIONS

#### A. General Description

A magnetometer with 37 channels, each having a first order gradiometer coil with a 7.1 cm baseline, was assumed in this computer simulation. The gradiometer coils are hexagonally aligned on a plane defined as the  $x - y$  plane with its origin equal to the center of this hexagon. The detector coil alignment is shown in Fig. 1. This alignment simulates the KRENIKON™ biomagnetic measurement system [14]. The  $z$ -direction is defined as the direction perpendicular to this detector-aligned-plane. The values of the spatial coordinates  $(x, y, z)$  are expressed in centimeters.

In this computer simulation, except in Section III-E, the horizontally layered infinite half-space conductor model [2] is assumed due to the ease of the calculation, and the boundary of the conductor is assumed to be perpendicular to the  $z$ -axis. Thus, only the  $x$  and  $y$  components of primary current vectors are considered, and their  $z$  components are assumed to be zero.

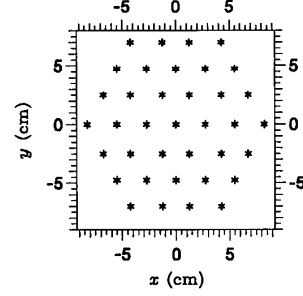


Fig. 1. Detector coil alignment assumed in computer simulation.

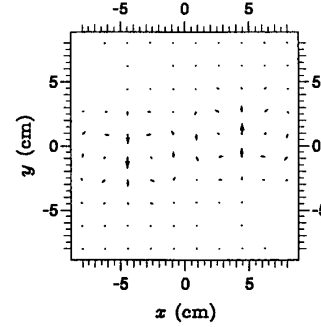


Fig. 2. Results of conventional minimum-norm reconstruction of the noiseless data. The current sources are located 4 cm below the detector-aligned-plane. The relative regularization parameter  $\varepsilon$  is set at  $10^{-5}$ .

Two-dimensional reconstruction of current sources is performed. The reconstruction area covers  $-8 \leq x \leq 8$  and  $-8 \leq y \leq 8$  and consists of  $10 \times 10$  pixels. It is assumed that the plane to be reconstructed has already been determined. This paper is not concerned with the determination of the plane containing biocurrent sources. Discussions regarding this determination can be found in [3], [15], [16].

#### B. Simulation for Low SNR Data

Two time-varying magnetic-field sources both of which are located 4 cm below the detector plane are assumed. One is a dipole rotated in the  $x$  and  $y$  plane with its moment intensity equal to 40 nA/mm. This is located at  $(-4.5, -1, -4)$ . The other is a fixed-orientation dipole located at  $(4.5, 1, -4)$ . The  $y$  component of its moment is sinusoidally modulated with its maximum intensity equal to 56 nA/mm, and the  $x$  component is fixed at zero. Let us choose the time instant at which the  $x$  and  $y$  components of the rotating-dipole moment happen to be  $(0, -40)$  nA/mm, and those of the fixed-orientation dipole moment happen to be  $(0, 40)$  nA/mm. The field distribution is calculated at each detector coil location at this time instant. The magnetic field data is obtained by subtracting the field strength at the gradiometer's upper-coil position from that at the lower-coil position.

The conventional minimum-norm reconstruction of the plane  $z = -4$  cm is performed using this noiseless field data. The results are shown in Fig. 2. In this reconstruction, (2) and (3) were used with the relative regularization parameter  $\varepsilon$  equal to  $10^{-5}$ . The relative regularization parameter  $\varepsilon$  indicates the

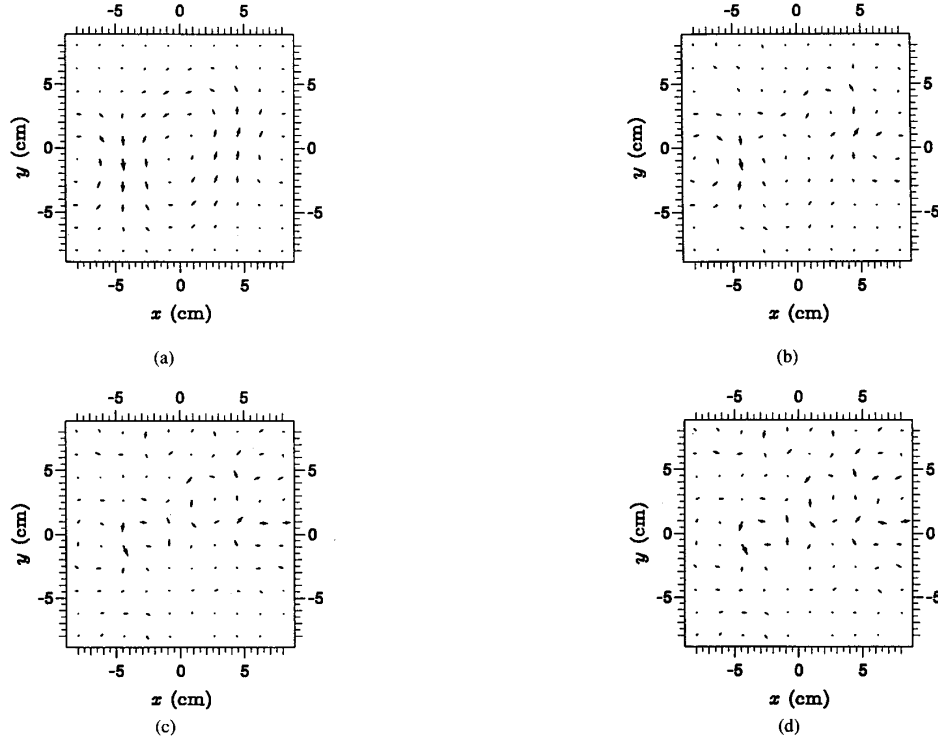


Fig. 3. Results of conventional minimum-norm reconstruction of noisy data (SNR = 2.4). The noisy data is generated by adding the uncorrelated Gaussian noise to the noiseless data whose reconstruction is shown in Fig. 2. The relative regularization parameter  $\varepsilon$  is equal to (a)  $10^{-1}$ , (b)  $10^{-2}$ , (c)  $10^{-3}$ , and (d)  $10^{-4}$ .

ratio of the regularization parameter  $\gamma$  to the largest eigenvalue of the matrix  $LL^T$ , i.e.,  $\varepsilon = \gamma/\lambda_0$ , where  $\lambda_0$  is the largest eigenvalue of  $LL^T$ .

Then, uncorrelated Gaussian noise with standard deviation equal to 27 fT is added to this noiseless data. The resultant SNR of the magnetic field data is equal to 2.4. The SNR is defined by the ratio of the root mean square of the signal magnetic field to the standard deviation of the Gaussian noise. The mean value is calculated over all 37 channels. The conventional minimum-norm reconstruction using (2) and (3) is performed on this noisy data with four values of the relative regularization parameter:  $\varepsilon = 10^{-1}$ ,  $10^{-2}$ ,  $10^{-3}$ , and  $10^{-4}$ . The results are shown in Fig. 3. Compared with Fig. 2, one can see that although the results obtained with  $\varepsilon = 10^{-1}$  and  $10^{-2}$  can, in some way, reconstruct the two current sources, the results with  $\varepsilon = 10^{-1}$  contain severe blur, and those with  $\varepsilon = 10^{-2}$  are considerably inaccurate. Compared again with Fig. 2, the results obtained with  $\varepsilon = 10^{-3}$ , and  $\varepsilon = 10^{-4}$  contain severe distortion, so they are almost meaningless.

The covariance matrix of the measured data is estimated from 1000 data generations; each generated data contain Gaussian noise with the same standard deviation as described above. That is, the  $(i, j)$  element of the covariance matrix,  $D_{ij}$ , is calculated using

$$D_{ij} = \frac{1}{K_c} \sum_{k=1}^{K_c} B_i(t_k) B_j(t_k). \quad (13)$$

Here,  $B_i(t_k)$  is the magnetic field measurement from the  $i$ th channel at the  $k$ th data generation, and  $K_c$  is equal to 1000. This simulates the data acquisition for 1 s, with a typical signal sampling interval of 1 ms. The Wiener reconstruction was performed using (3) and (12) with four values of the relative regularization parameter:  $\varepsilon = 10^{-1}$ ,  $\varepsilon = 10^{-2}$ ,  $\varepsilon = 10^{-3}$ , and  $\varepsilon = 10^{-4}$ . The results are shown in Fig. 4. In this figure, the two current sources can be reconstructed with any of the  $\varepsilon$  values. These results indicate that the Wiener reconstruction is much more tolerant to the choice of the regularization parameters than the minimum-norm method. Moreover, as a result of this tolerance, we can use smaller regularization parameters, and thus obtain less blurred reconstruction. This is shown by the comparison between Fig. 3(a) and Fig. 4(b), (c), or (d), and this comparison clearly demonstrates the effectiveness of the Wiener method.

The average-intensity distribution,  $\langle f_i^2 \rangle$  ( $i = 1, 2, \dots, 2N$ ), is reconstructed from this covariance matrix using (3) and (9). The results with the same four values of the relative regularization parameter are shown in Fig. 5. Here, two current sources are clearly reconstructed, and the results are also tolerant of the choice of the regularization parameter. Note that the reconstructed rotating dipole located at  $(-4.5, -1, -4)$  has its moment directed at  $45^\circ$  to the  $+x$ -axis, because the average intensities of the  $x$  and  $y$  moment components are equal in this rotating dipole.

Next, we investigated the effect of the accuracy in estimating the measured-data covariance matrix on the final

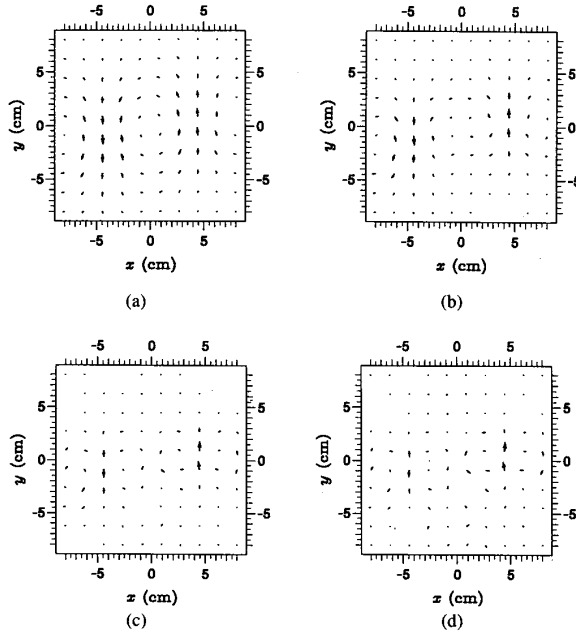


Fig. 4. Results of Wiener reconstruction of the noisy data with (a)  $\varepsilon = 10^{-1}$ , (b)  $\varepsilon = 10^{-2}$ , (c)  $\varepsilon = 10^{-3}$ , and (d)  $\varepsilon = 10^{-4}$ .

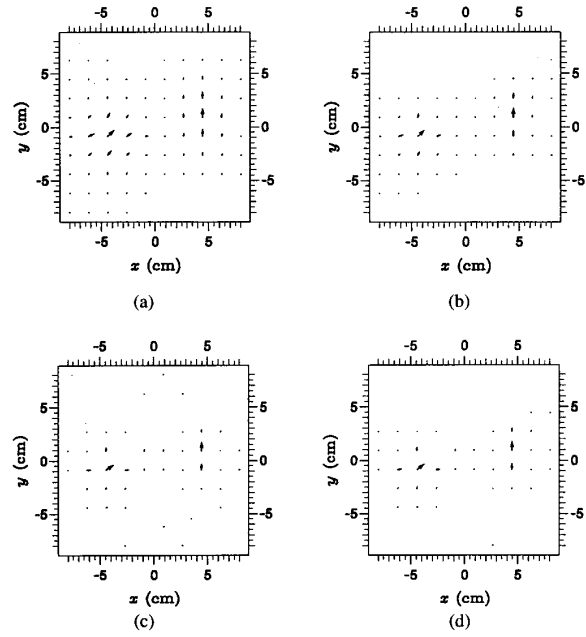


Fig. 5. Results of average-intensity reconstruction of the noisy data with (a)  $\varepsilon = 10^{-1}$ , (b)  $\varepsilon = 10^{-2}$ , (c)  $\varepsilon = 10^{-3}$ , and (d)  $\varepsilon = 10^{-4}$ .

reconstructed results. The covariance matrices were estimated from 500, 250, and 125 data generations, i.e., the matrices were calculated with  $K_c$  in (13) equal to 500, 250, and 125. Naturally, the larger the  $K_c$ , the more accurate is the estimation. The results of the Wiener reconstruction with  $\varepsilon = 10^{-2}$  using these covariance matrices are shown in Fig. 6. The results using the covariance matrix calculated with  $K_c = 500$  are shown in Fig. 6(a), the results when  $K_c = 250$  are shown in Fig. 6(b), and the results when  $K_c = 125$  are shown in Fig. 6(c). Note that the results when  $K_c = 1000$  are shown in Fig. 4(b).

Comparing Fig. 6 with Fig. 4(b), we see that the covariance matrix calculated with  $K_c = 500$  gives almost the same quality of results as those shown in Fig. 4(b). The results obtained using the covariance matrix calculated with  $K_c = 250$ , however, contain a slight inaccuracy, and those obtained using the covariance matrix calculated with  $K_c = 125$  contain severe distortion. Obviously, the accuracy in estimating the covariance matrix affects the tolerance of the value of the regularization parameter. This point will be discussed in Section IV.

### C. Simulation for High SNR Data

In this simulation, the moments of the two current sources are set at ten times greater values than those assumed in Section III-B. That is, the moment intensity of the rotating dipole located at  $(-4.5, -1, -4)$  was 400 nA/mm and the maximum moment of the fixed-orientation dipole located at  $(4.5, 1, -4)$  is 560 nA/mm. The magnetic field data were calculated assuming that the rotating and the fixed-orientation dipole moments are  $(0, 400)$  nA/mm and  $(0, -400)$  nA/mm, respectively. Since noise with standard deviation equal to 27 fT

was added to the calculated magnetic field data, the resultant signal-to-noise ratio was 24.

The results obtained using the minimum-norm, the Wiener, and the average-intensity methods are shown in Fig. 7(a), (b), and (c), respectively. All of these results were obtained using  $\varepsilon = 10^{-4}$ . The results show that the minimum-norm method can obtain results with the same quality as the Wiener method. Thus, for such high SNR data, the Wiener and the average-intensity methods do not have clear advantages.

### D. Simulation of Reconstructing Deeply Located Sources

Next, the two sources were located 8 cm below the detector plane. That is, the coordinates of the rotating dipole were  $(-4.5, -1, -8)$  and those of the fixed dipole were  $(4.5, 1, -8)$ . The moment intensity of the rotating dipole was set at 120 nA/mm and the maximum moment of the fixed-orientation dipole at 170 nA/mm. The magnetic field data were calculated assuming that the rotating and the fixed-orientation dipole moments are  $(0, 120)$  nA/mm and  $(0, -120)$  nA/mm, respectively. The uncorrelated noise with the same standard deviation as was used in the preceding sections was added to the calculated magnetic field data. The resulting SNR is 2.1.

Fig. 8 shows that the results obtained by the minimum-norm method with  $\varepsilon$  equal to  $10^{-1}$ ,  $10^{-2}$  and  $10^{-3}$ . The minimum-norm method could reconstruct the two current sources only when  $\varepsilon = 10^{-1}$ , and failed to reconstruct them with  $\varepsilon \geq 10^{-2}$ . The reconstructed results obtained using the Wiener method with  $\varepsilon = 10^{-1}$ ,  $\varepsilon = 10^{-2}$  and  $\varepsilon = 10^{-3}$  are shown in Fig. 9. The Wiener method can still reconstruct the two current sources, although the reconstructed results with  $\varepsilon = 10^{-1}$  and with  $\varepsilon = 10^{-2}$  contain significant blur, and the positions of the two sources reconstructed with  $\varepsilon = 10^{-3}$  are somewhat

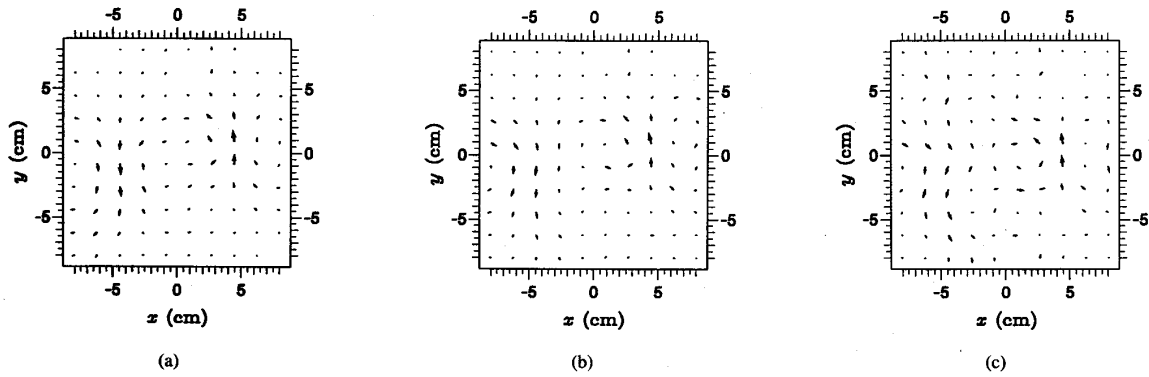


Fig. 6. Results of Wiener reconstruction of the noisy data with  $\varepsilon$  equal to  $10^{-2}$ . Here, covariance matrices calculated from (a) 500 data generation, (b) 250 data generation, and (c) 125 data generation, are used.

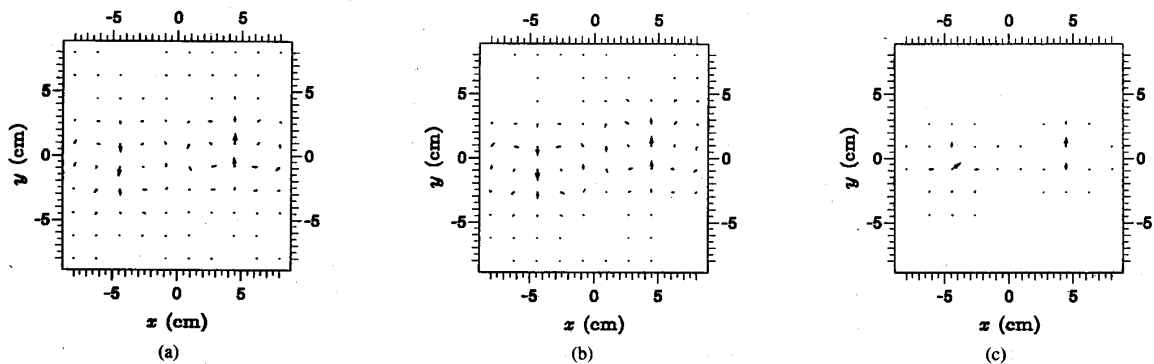


Fig. 7. Results of reconstruction experiments for high SNR data (SNR = 24). Results obtained using (a) minimum-norm reconstruction with  $\varepsilon = 10^{-4}$ , (b) Wiener reconstruction with  $\varepsilon = 10^{-4}$ , and (c) average-intensity reconstruction with  $\varepsilon = 10^{-4}$ .

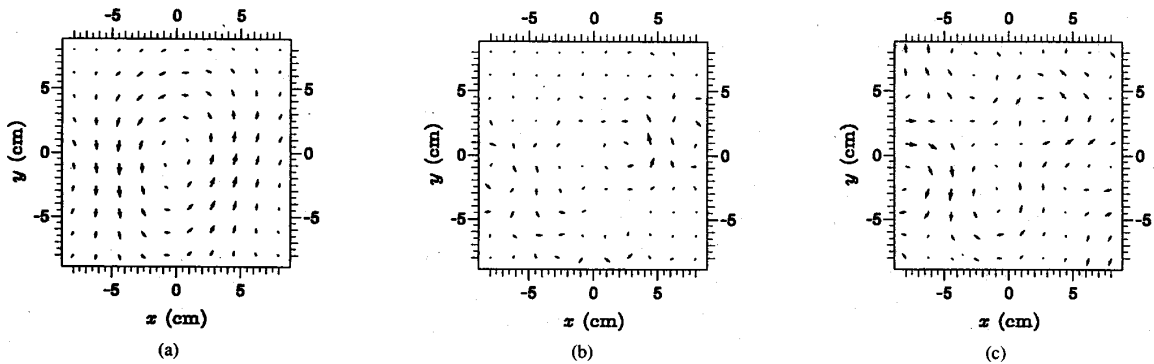


Fig. 8. Results of reconstructing deeply located sources obtained using minimum-norm reconstruction with (a)  $\varepsilon = 10^{-1}$ , (b)  $\varepsilon = 10^{-2}$ , and (c)  $\varepsilon = 10^{-3}$ . The current sources are located 8 cm below the detector-aligned-plane, and the SNR of the magnetic field data is equal to 2.1.

inaccurate. Comparison between Figs. 8 and 9 shows that the Wiener method also can give better results in this case. The results obtained by the average-intensity reconstruction are shown in Fig. 10. The figure shows that the two current sources are clearly reconstructed at the correct position, and this method can provide less blurred reconstruction for the same three values of  $\varepsilon$ , compared with the results obtained using the Wiener method.

Next, the case of an extremely low signal-to-noise ratio was simulated. The moment intensities of the current sources were set at the same values as used in Section III-B. The resultant SNR was 0.7 in this case, and the reconstructed results obtained using the minimum-norm and the Wiener methods with  $\varepsilon = 10^{-1}$  are shown in Fig. 11(a) and (b). Not only the minimum-norm method, but also the Wiener method failed to reconstruct the two current sources. The results obtained

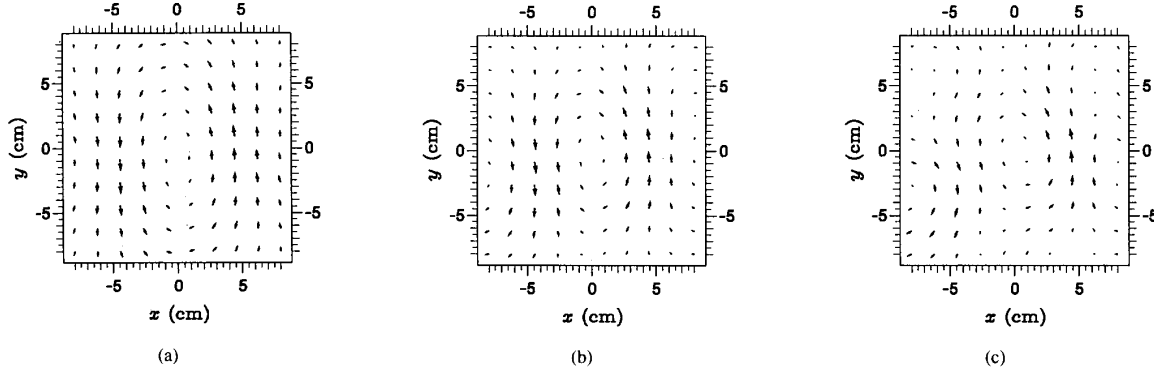


Fig. 9. Results of reconstructing deeply located sources obtained using Wiener reconstruction with (a)  $\varepsilon = 10^{-1}$ , (b)  $\varepsilon = 10^{-2}$ , and (c)  $\varepsilon = 10^{-3}$ .

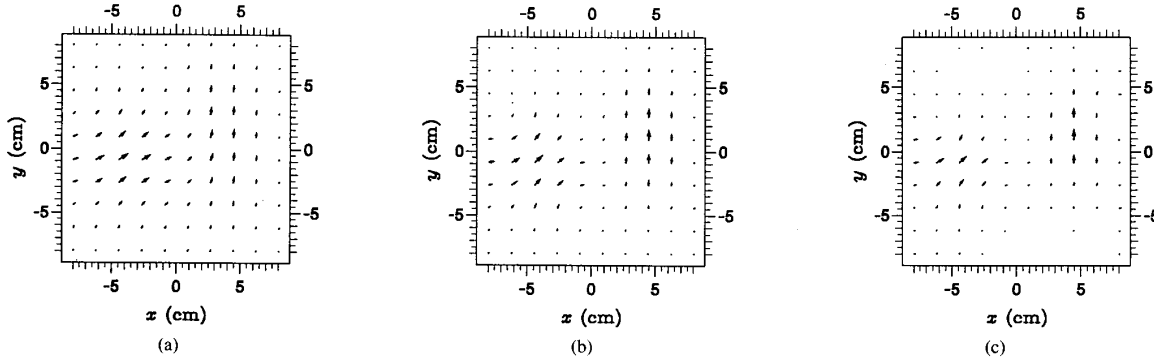


Fig. 10. Results of reconstructing deeply located sources obtained using average-intensity reconstruction with (a)  $\varepsilon = 10^{-1}$ , (b)  $\varepsilon = 10^{-2}$ , and (c)  $\varepsilon = 10^{-3}$ .

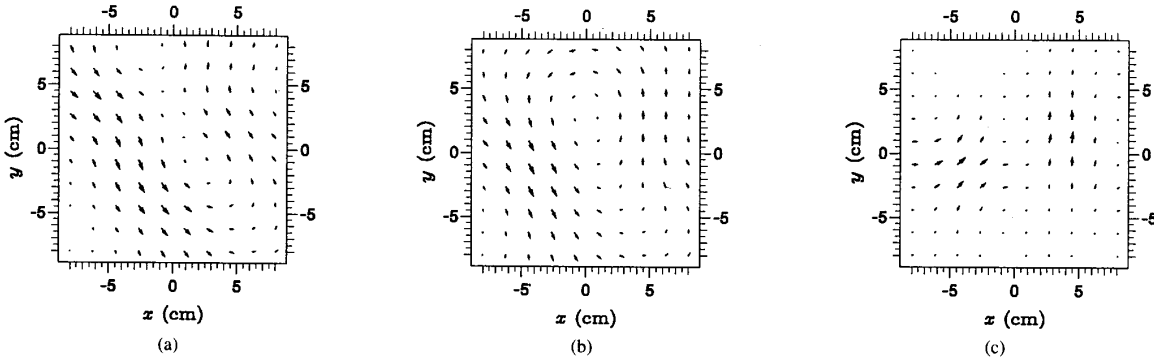


Fig. 11. Results of experiments for extremely low SNR data. The current sources are located 8 cm below the detector-aligned-plane, and the SNR of the magnetic field data is equal to 0.7. The results obtained using (a) minimum-norm reconstruction with  $\varepsilon = 10^{-1}$ , (b) Wiener reconstruction with  $\varepsilon = 10^{-1}$ , and (c) average-intensity reconstruction with  $\varepsilon = 10^{-2}$ .

using the average-intensity method with  $\varepsilon = 10^{-2}$  are shown in Fig. 11(c). The average-intensity method can reconstruct the current sources at the correct position, and this demonstrates the advantage of the average-intensity reconstruction over the Wiener method in the case of extremely low SNR.

#### E. Simulation Using Spherical Homogeneous Conductor

This section describes a computer simulation identical to that in Section III-B, except that the spherical homogeneous conductor model with its center located at (0, 0, -12) was

used. This spherical homogeneous conductor is often used for solving the neuromagnetic inverse problem. The lead field was calculated using the equation reported by Sarvas [2]. The signal-to-noise ratio of the magnetic field data was 3.0.

First, the minimum-norm method was applied to this data with  $\varepsilon = 10^{-1}$ ,  $\varepsilon = 10^{-2}$ ,  $\varepsilon = 10^{-3}$ , and  $\varepsilon = 10^{-4}$ , and only the case with  $\varepsilon = 10^{-1}$  was found to be able to reconstruct the two current sources. The results are shown in Fig. 12(a). The Wiener method and the average-intensity method could reconstruct the two sources with any of the above four values

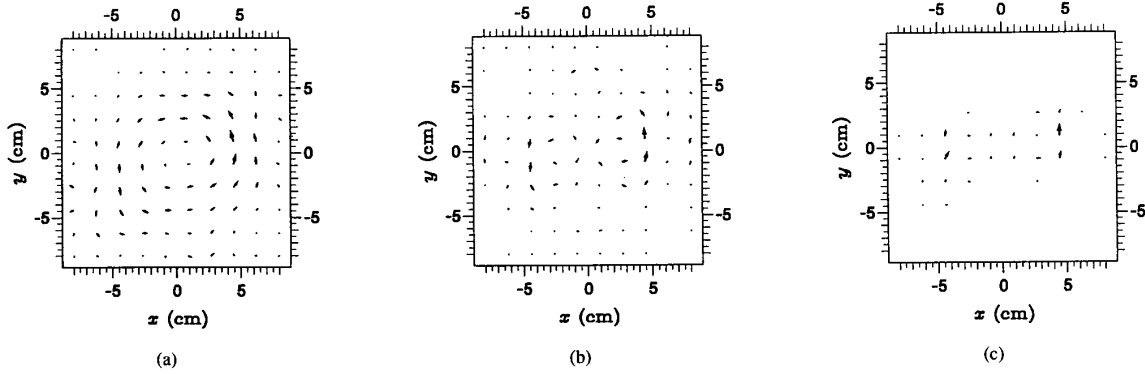


Fig. 12. Results of experiments using the spherical homogeneous conductor model. The current sources are located 4 cm below the detector-aligned-plane, and the SNR of the magnetic field data is equal to 3.0. The results obtained using (a) minimum-norm reconstruction with  $\varepsilon = 10^{-1}$ , (b) Wiener reconstruction with  $\varepsilon = 10^{-4}$ , and (c) average-intensity reconstruction with  $\varepsilon = 10^{-4}$ .

of  $\varepsilon$ , and the least blurred reconstruction was obtained with the smallest  $\varepsilon$ , i.e.,  $\varepsilon = 10^{-4}$ . The results in this case are shown in Fig. 12(b) and (c). These results are very similar to those obtained in Section III-B. The results shown in Fig. 12 demonstrate that the Wiener and the average-intensity methods are also effective for the spherical homogeneous conductor model.

#### IV. DISCUSSIONS

One problem with the proposed methods is that they require prior information regarding the noise covariance matrix. If the noise can be assumed as uncorrelated Gaussian noise, the noise covariance matrix becomes a diagonal matrix, and a diagonal term is equal to a channel's noise variance. In such cases, it is not difficult to obtain the information regarding the noise covariance matrix because each channel's noise variance can be easily measured in advance of the reconstruction.

It has been pointed out, however, that the noise due to external sources is spatially correlated in the data measured by a multichannel magnetometer [17]. In such cases, the estimation of the noise covariance needs to find the portion of the data which contains only noise information, and not signal information [17]. In many cases of neuromagnetic measurements, it is not difficult to find such data portions. For example, the data before the application of stimuli can be used to calculate the covariance matrix in measurements of evoked neuromagnetic fields [18]. In measurements of epileptic signals, the data anywhere except at epileptic spikes can be used [19].

This paper is not the first one that proposes applying the Wiener reconstruction method to solve the biomagnetic inverse problem. Smith *et al.* introduced the Wiener method to reconstruct biocurrent distributions [20]. In [20], however, no method of estimating the source-distribution covariance  $S$  is described. Instead, they proposed introducing ad hoc assumptions regarding noise and source covariance matrices. It is, however, difficult to prove the validity of these assumptions [21]. Thus, in applying their method to actually measured data [22], they simply used minimum-norm reconstruction derived from the Wiener method by assuming that the noise and signal-

source covariance matrices are equal to diagonal matrices. In the method proposed here, the Wiener reconstruction is reformulated using the measured data covariance matrix  $D$  and the lead field matrix  $L$ . This reformulation makes it possible to utilize the time information regarding the time-varying magnetic source distributions in this method.

In the computer simulation described in the preceding section, it was shown that the proposed Wiener and average-intensity reconstruction methods are considerably less sensitive to the choice of the value of the regularization parameter, but it was also shown that the tolerance of this value is affected by the accuracy in estimating the measured-data covariance matrix, i.e., by the number of data used to calculate the covariance matrix.

It is, however, not easy to determine the number needed to give accurate estimation of the covariance matrix, because this number depends on the various conditions in the data acquisition, such as the amplitude of the noise in the measured data or the distances between the current sources and detector coils. Thus, the effectiveness of the proposed methods must finally be evaluated by applying them to various kinds of actual source localization problems. Some biomagnetic fields are generated by rapidly decaying sources, and the proposed methods may not be effective in such cases, because a sufficient number of data to give accurate covariance matrix estimation may not be obtained in such cases.

Finally, it should be pointed out that the Wiener method requires approximately twice the computation time needed for the minimum-norm method, because it requires inversion of an  $M \times M$  matrix twice. Typical numbers of channels  $M$  for currently available magnetometers range from 37 to 62, and an additional inversion of a  $62 \times 62$  matrix causes no serious problem, considering the computational power of a commercially available small computer. This, however, may cause some problems if the number of channels increases in the future and if quasi-real time processing is required.

#### V. CONCLUSION

This paper proposes two methods suitable for reconstructing bioelectric current distributions from low SNR biomag-



netic measurements. One method is reconstruction of average-current-intensity distributions in which current intensity distributions averaged over the period of calculating the measured-data covariance matrix are reconstructed. This method is effective for extremely low SNR cases, although it cannot reconstruct the orientation of each current element at each time instant. The second method is the Wiener reconstruction based on the estimated source covariance matrix. This method can reconstruct the biocurrent distribution with its orientation at each time instant. Compared with the conventional minimum-norm reconstruction, the Wiener method is much less sensitive to the choice of the value of the regularization parameter, resulting in a method that is effective in low SNR cases. Results of computer simulation demonstrate the effectiveness of both methods.

#### ACKNOWLEDGMENT

The authors wish to acknowledge Dr. A. Oppelt for the discussion concerning the use of time information in the estimation of biocurrent distributions. K. Sekihara particularly thanks Mr. H. Bruder for his assistance in computer programming.

#### REFERENCES

- [1] M. S. Hämäläinen and R. J. Ilmoniemi, "Interpreting measured magnetic fields of the brain: Estimates of current distributions," Helsinki University of Technology, Rep. TKK-F-A559, 1984.
- [2] J. Sarvas, "Basic mathematical and electromagnetic concepts of the biomagnetic inverse problem," *Phys. Med. Biol.*, vol. 32, pp. 11–22, 1987.
- [3] R. Graumann, "The reconstruction of current densities," Helsinki University of Technology, Rep. on Biomagn. Localization and 3-D Modeling, TKK-F-A689, 1991, pp. 172–186.
- [4] R. M. Chapman, "Spontaneous EEG/MEG: Current status of biomagnetic research," in *8th Int. Conf. Biomagn.*, Münster, Germany, p. 17, Aug. 1991.
- [5] S. Sato, "Current status of biomagnetic research in epileptology," in *8th Int. Conf. Biomagn.*, Münster, Germany, p. 31, Aug. 1991.
- [6] C. L. Lawson and R. J. Hanson, *Solving Least Squares Problems*. Englewood Cliffs, NJ: Prentice-Hall, 1974.
- [7] C. W. Groetsch, *The Theory of Tikhonov Regularization for Fredholm Equations of The First Kind*. London: Pitman, 1984.
- [8] H. C. Andrews and B. R. Hunt, *Digital Image Restoration*. Englewood Cliffs, NJ: Prentice-Hall, 1977.
- [9] A. M. Thompson and J. Kay, "On some Bayesian choices of regularization parameter in image restoration," *Inverse Problem*, vol. 9, pp. 749–761, 1993.
- [10] A. M. Thompson, J. C. Brown, J. W. Kay, and D. M. Titterton, "A study of methods of choosing the smoothing parameter in image restoration by regularization," *IEEE Trans. Pattern Anal. Machine Intell.*, vol. 13, pp. 326–339, 1991.
- [11] S. F. Gull and G. J. Daniell, "Image reconstruction from incomplete and noisy data," *Nature*, vol. 272, pp. 686–700, 1978.
- [12] W. H. Press, S. A. Teukolsky, W. T. Vetterling, and B. P. Flannery, *Numerical Recipes*, 2nd ed. Cambridge, MA: Cambridge Univ. Press, 1993.
- [13] W. K. Pratt, *Digital Image Processing*. New York: Wiley, 1978.
- [14] S. Schneider, E. Hoenig, H. Reichenberger, K. Abraham-Fuchs, G. Daalmans, W. Moshage, A. Oppelt, G. Röhrlein, H. Stefan, J. Vieth, A. Weikl, and A. Wirth, "Multichannel biomagnetic system for high-resolution functional studies of brain and heart," *Radiology*, vol. 176, pp. 825–830, 1990.
- [15] B. Scholz, K. Sekihara, and R. Killmann, "Lead field reconstruction of biomagnetic current densities in the current supporting planes," in *Proc. 14th Annu. Int. Conf. IEEE Eng. in Med. and Biol. Soc.*, pp. 2176–2177, Paris, France, Nov. 1992.
- [16] A. A. Ioannides, J. P. R. Bolton, and C. J. S. Clark, "Continuous probabilistic solutions to the biomagnetic inverse problem," *Inverse Problem*, vol. 6, pp. 523–542, 1990.
- [17] K. Sekihara, Y. Ogura, and M. Hotta, "Maximum likelihood estimation of current dipole parameters for data obtained using multichannel magnetometer," *IEEE Trans. Biomed. Eng.*, vol. 36, pp. 558–562, 1992.
- [18] K. Sekihara, F. Takeuchi, S. Kuriki, and H. Koizumi, "Reduction of brain noise influence in evoked neuromagnetic source localization using noise spatial correlation," *Phys. Med. Biol.*, vol. 39, pp. 937–946, 1994.
- [19] K. Abraham-Fuchs, K. Sekihara, H. Stefan, and E. Hellstrand, "Separation of epileptic spike activity from background rhythmic brain activity using noise spatial coherence," in *Proc. 14th Annu. Int. Conf. IEEE Eng. in Med. and Biol. Soc., Satellite Symp. Neurosci. and Technol.*, pp. 8–14, 1992.
- [20] W. E. Smith, W. J. Dallas, W. H. Kullmann, and H. A. Schlitt, "Linear estimation theory applied to the reconstruction of a 3-D vector current distribution," *App. Opt.*, vol. 29, pp. 658–667, 1990.
- [21] H. A. Schlitt, "A Fourier transform technique for estimating bioelectric currents from magnetic field measurements," Ph.D. dissertation, Univ. of Arizona, 1992.
- [22] W. H. Kullmann, K. D. Jandt, K. Rehm, H. A. Schlitt, W. J. Dallas, and W. E. Smith, "A linear estimation approach to biomagnetic imaging," *Advances in Biomagnetism*, S. J. Williamson, M. Hoke, G. Stroink, and M. Kotani, Eds. New York: Plenum Press, 1989, pp. 571–574.



**Kensuke Sekihara** (M'88) received the M.S. degree in 1976 and the Ph.D. degree in 1987, both from the Tokyo Institute of Technology.

Since 1976, he has worked with Central Research Laboratory, Hitachi, Limited, Tokyo, Japan. He was a Visiting Research Scientist at Stanford University, Stanford, CA from 1985 to 1986, and at Basic Development, Siemens Medical Engineering, Erlangen, Germany, from 1991 to 1992. His research interests are image reconstruction and processing algorithms, the biomagnetic inverse problem, statistical estimation theory, and *in vivo* measurements of brain functions. He is currently a Senior Research Scientist at Hitachi Central Research Laboratory. Dr. Sekihara is a Member of the IEEE Medicine and Biology Society and the Society of Magnetic Resonance.



**Bernhard Scholz** received the M.S. degree in 1974 and the Ph.D. degree in 1978, both in physics, from the University of Heidelberg, Germany. His theses were on experimental and theoretical elementary particle physics for the M.S. and the Ph.D. degrees, respectively.

After receiving the Ph.D. degree, he worked as an Assistant in theoretical physics. In 1986, he joined the CAD group for VLSI design of the Corporate Research Center of Siemens in Munich, Germany. Since 1987, he has worked in the Simulation Department of the Basic Research Laboratory at the Siemens Medical Engineering Division in Erlangen, Germany. His current interests are in simulations of complex imaging systems and image reconstruction.